

5015

# Simulation of Steamflooding With Distillation and Solution Gas

K. H. COATS  
MEMBER SPE-AIME

INTERCOMP RESOURCE DEVELOPMENT AND  
ENGINEERING, INC.  
HOUSTON, TEX.

## ABSTRACT

This paper describes a three-dimensional numerical model for simulating steam-injection processes. The model accounts for solution gas and steam distillation of oil. The relative-permeability treatment presented includes a flexible but simple representation of temperature dependence and a history-dependent hysteresis in gas relative permeability. Since computational stability is a major difficulty in steamflood simulation, an implicit treatment of transmissibilities and capillary pressure is presented in detail. Model applications include comparisons with laboratory data, sensitivity experiments, and a field steam-injection test.

## INTRODUCTION

Shutler<sup>1,2</sup> and Abdalla and Coats<sup>3</sup> described two-dimensional, three-phase flow numerical models for simulating steam-injection processes. Weinstein *et al.*<sup>4</sup> described a one-dimensional model that accounted for steam distillation of oil. Coats *et al.*<sup>5</sup> described a three-dimensional steamflood model that neglected steam distillation of oil, release of solution gas at elevated temperatures, and temperature dependence of relative permeability. This paper describes an extended formulation that includes these three phenomena and uses a more implicit treatment of capillary pressures and transmissibilities in the fluid-saturation calculations. The extended formulation represents a step toward a fully compositional thermal model without incurring the computational expense of the latter.

The relative-permeability treatment described includes a rather flexible but simple representation of temperature dependence and incorporates a hysteresis in gas-phase relative permeability that varies with the historical maximum grid-block gas saturation. The phase-behavior representation is the weakest element of this work. We have found insufficient data relative to PVT behavior of a heavy-oil/steam system to justify sophisticated schemes of the type used in isothermal hydrocarbon

systems. The PVT treatment presented is the simplest we could construct subject to the objectives of "directional correctness," reasonable quantitative accuracy, and ability to obtain required parameters from laboratory data either normally available or readily determinable.

Model results presented include a comparison with laboratory data for a steamflood of a distillable oil; sensitivity results indicating effects and relative importance of various types of input data; and a comparison between calculated and observed injection rates for a Cold Lake (Alta.) steam-injection test. The latter is of interest in regard to reservations we have had regarding a model's ability to predict steam-injection rates into virtually immobile oil (100,000 cp). The field-test data showed initial and sustained steam-injection rates of 1,400 STB/D (cold-water equivalent). We discuss several reservoir-fluid parameters that had little effect and one independently measured parameter that had a pronounced effect on the calculated injection rate.

## MODEL DESCRIPTION

The model consists of seven equations expressing conservation of energy, conservation of mass, and constraints on sums of liquid and gas phase mol fractions. The mass-conservation equations apply to water and to each of three hydrocarbon components. In finite-difference form these equations are the following.

Mass Balances on Hydrocarbon Components

$$\frac{V}{\Delta t} \delta (\phi \rho_o S_o x_i + \phi \rho_g S_g y_i) = \Delta [T_o x_i (\Delta p_o - \gamma_o \Delta Z) + T_g y_i (\Delta p_g - \gamma_g \Delta Z)] - q_o \rho_o x_i - q_g \rho_g y_i, \quad i=1, 2, 3, \dots \quad (1-3)$$

Mol Fraction Constraint

$$\delta x_1 + \delta x_2 + \delta x_3 = 0 \dots \dots \dots (4)$$

Original manuscript received in Society of Petroleum Engineers office Oct. 15, 1974. Paper accepted for publication Feb. 13, 1975. Revised manuscript received June 30, 1976. Paper (SPE 5015) was first presented at the SPE-AIME 49th Annual Fall Meeting, held in Houston, Oct. 6-9, 1974. © Copyright 1976 American Institute of Mining, Metallurgical, and Petroleum Engineers, Inc.

Mass Balance on H<sub>2</sub>O

$$\frac{V}{\Delta t} \delta(\phi \rho_w S_w + \phi \rho_g S_g y_s) = \Delta [T_w (\Delta p_w - \gamma_w \Delta Z) + T_g y_s (\Delta p_g - \gamma_g \Delta Z)] - q_w \rho_w - q_g \rho_g y_s \dots (5)$$

Energy Balance

$$\frac{V}{\Delta t} \delta[\phi(\rho_w S_w U_w + \rho_o S_o U_o + \rho_g S_g U_g) + (1-\phi)(\rho C_p)_R T] = \Delta(T_H \Delta p) + \Delta(T_c \Delta T) - q_L - q_H \dots (6)$$

Gas Mol Fraction Constraint

$$\delta y_1 + \delta y_2 + \delta y_s = 1 - y_{1n} - Y_{2n} - Y_{sn} \dots (7)$$

Several of these equations and the terminology are described in detail in an earlier paper.<sup>5</sup> The Nomenclature further describes the terminology.

Water- and gas-phase pressures are related to oil pressure through capillary pressure as

$$p_w = p - P_{cwo} \quad p_g = p + P_{cgo} \dots (8)$$

If no gas phase is present, Eq. 7 is replaced by

$$\delta S_g = -S_{gn}$$

Densities, viscosities, relative permeabilities, and enthalpies in the transmissibilities are dated explicitly at time level *n*. Relative permeabilities and gas-phase viscosity are weighted 100 percent upstream while water and oil viscosities may be weighted upstream or taken as arithmetic interblock averages. Temperature in the conduction term  $\Delta(T_c \Delta T)$  is expressed explicitly.

The hydrocarbon-component liquid and gas mol fractions are related through equilibrium *K* values:

$$y_1 = K_1(p, T) x_1 \quad y_2 = K_2(p, T) x_2 \dots (9)$$

Component 1 represents the light ends or solution gas, Component 2 represents the distillable portion of the oil, and Component 3 represents the nonvolatile heavy ends. The steam mol fraction, *y<sub>s</sub>*, is *p<sub>sat</sub>/p*, where *p<sub>sat</sub>* is steam saturation pressure, a single-valued function of temperature.

Eqs. 1 through 7 are seven equations in the seven unknowns *x<sub>1</sub>*, *x<sub>2</sub>*, *x<sub>3</sub>*, *S<sub>g</sub>*, *S<sub>w</sub>*, *T*, and *p*. All other variables or coefficients can be expressed in terms of one or more of these unknowns. Water molar

density, *ρ<sub>w</sub>*, is dependent on temperature and pressure as

$$\rho_w(p, T) = \rho_w(T) (1 + c_w(p - p_{sat})), \dots (10)$$

where *ρ<sub>w</sub>(T)* is water molar density at temperature *T* and steam saturation pressure *p<sub>sat</sub>(T)*. Gas-phase molar density is calculated as

$$\rho_g = \frac{p}{zRT} \times 5.6146, \dots (11)$$

where *z* is calculated as a mol-weighted average of hydrocarbon gas and steam *z* factors. The hydrocarbon-gas *z* factor is entered as a two-dimensional tabular function of total pressure and temperature. Interpolation in this table gives *z<sub>gas</sub>*. The steam *z* factor (*z<sub>s</sub>*) is obtained at a temperature from the steam tables. The gas-phase *z* factor used in Eq. 11 is then calculated as

$$z = y_s z_s + (1 - y_s) z_{gas} \dots (12)$$

Oil-phase molar density is entered as a single-valued function of Component 3 mol fraction at original reservoir pressure and temperature. Denoting this value by *ρ<sub>o</sub>(x<sub>3</sub>)*, the value of *ρ<sub>o</sub>* is then calculated as

$$\rho_o(p, T, x_3) = \rho_o(x_3) (1 - C_{TO}(T - T_i) + c_o(p - p_i)) \dots (13)$$

Water and steam internal energies, *l<sub>w</sub>* and *l<sub>s</sub>*, are taken directly from the steam tables as single-valued functions of temperature. Oil- and gas-phase internal energies are calculated as

$$U_o = (x_1 C_{p1} + x_2 C_{p2} + x_3 C_{p3}) T, \dots (14a)$$

and

$$U_g = (y_1 C_{p1} + y_2 C_{p2}) T + y_s U_s, \dots (14b)$$

where specific heats *C<sub>p1</sub>*, *C<sub>p2</sub>*, and *C<sub>p3</sub>* are assumed to be constants.

The hydrocarbon-component equilibrium *K* values are entered as two-dimensional tabular functions of temperature and pressure: no dependence on composition is represented. Stock-tank gas and oil compositions are calculated by a flash calculation using wellstream composition and specified values of *K<sub>1</sub>* and *K<sub>2</sub>* at stock-tank conditions.

Water viscosity is represented as a single-valued function of temperature. Hydrocarbon gas viscosity (*μ<sub>gas</sub>*) is entered as a two-dimensional tabular function of temperature and pressure. Steam viscosity is represented as a single-valued function of

temperature. Gas-phase viscosity is then calculated as

$$\mu_g = y_s \mu_s + (1 - y_s) \mu_{\text{gas}} \dots (15)$$

Oil viscosity is calculated as the product of a compositional-dependent factor,  $\mu_o(x_3)$ , and a temperature-dependent factor,  $\mu_o(T)$ :

$$\mu_o(T, x_3) = \mu_o(x_3) \mu_o(T) \dots (16)$$

The factor  $\mu_o(x_3)$  is 1.0 at  $x_3 = x_{3i}$  and varies with  $x_3$  as specified in tabular form. Thus,  $\mu_o(T)$  is the viscosity of original reservoir oil as a function of temperature. Porosity is treated as a function of pressure according to

$$\phi = \phi_i (1 + c_r (p - p_i)) \dots (17)$$

The formation thermal conductivity,  $K_R$ , incorporated in  $T_c$  in Eq. 6 is assumed constant and independent of fluid saturations. Overburden thermal conductivity is assumed constant and independent of fluid flow rate in the formation. Overburden heat loss is calculated as described in Ref. 5.

Eqs. 1 through 7 are solved in three stages. First, a pressure equation is obtained by eliminating all unknowns except  $\delta p$ . Solution of this equation is followed by solution of the system (Eqs. 1 through 7) for the other six unknowns, including  $\delta S_w$  and  $\delta S_g$ . Second, the water- and oil-phase mass balance equations are rewritten with implicit capillary pressure and implicit transmissibilities. These two equations are solved simultaneously for revised values of  $\delta S_w$  and  $\delta S_g$ . Third, production rates of water, oil, and gas phases from each producing grid block are adjusted to reflect implicit or time-level  $n + 1$  values of mobilities. The following sections describe each of these stages.

#### PRESSURE EQUATION

The left-hand sides of Eqs. 1 through 7 can be expanded in terms of the seven unknowns  $\delta x_1$ ,  $\delta x_2$ ,  $\delta x_3$ ,  $\delta S_g$ ,  $\delta S_w$ ,  $\delta T$ , and  $\delta p$  as described in Ref. 5. All pressures in the right-hand-side flow terms are expressed implicitly at time level  $n + 1$ , except that capillary pressures are held explicit at time level  $n$ . The seven equations can then be represented by

$$C \underline{P} = I \underline{Y} + \underline{R}, \dots (18)$$

where  $I$  is the identity matrix and  $C = (C_{ij})$  is the matrix of coefficients resulting from expansions of the time differences on the left-hand side of Eqs. 1 through 7. The column vectors  $\underline{P}$  and  $\underline{Y}$  are

$$\underline{P} = \begin{bmatrix} \delta x_1 \\ \delta x_2 \\ \delta x_3 \\ \delta S_g \\ \delta S_w \\ \delta T \\ \delta p \end{bmatrix} \quad \underline{Y} = \begin{bmatrix} \Delta(T_1 \Delta \delta p) \\ \Delta(T_2 \Delta \delta p) \\ \Delta(T_3 \Delta \delta p) \\ 0 \\ \Delta(T_{H_2O} \Delta \delta p) \\ \Delta(T_H \Delta \delta p) \\ 0 \end{bmatrix} \dots (19)$$

The elements  $R_i$  of the column vector  $\underline{R}$  are

$$R_i = \Delta [ T_o x_i (\Delta p_{on} - \gamma_o \Delta Z) + T_g y_i (\Delta p_{gn} - \gamma_g \Delta Z) ] - (q_o \rho_o x_i + q_g \rho_g y_i) n,$$

$$i = 1, 2, 3$$

$$R_4 = 0$$

$$R_5 = \Delta [ T_w (\Delta p_{wn} - \gamma_w \Delta Z) + T_g y_s (\Delta p_{gn} - \gamma_g \Delta Z) ] - (q_w \rho_w + q_g \rho_g y_s) n$$

$$R_6 = \Delta (T_H \Delta p_n) + \Delta (T_c \Delta T_n) - q_{Ln} - q_{Hn}$$

$$R_7 = 1 - y_{1n} - y_{2n} - y_{sn} \dots (20)$$

Application of Gaussian elimination to the system of seven equations (Eqs. 18), as described in Ref. 5, results in a pressure equation,

$$c \delta p = \Delta (T \Delta \delta p) + r \dots (21)$$

This is a simplified representation in that the actual form of the Laplacian  $\Delta (T \Delta \delta p)$  is the sum

$$\alpha_1 \Delta (T_1 \Delta \delta p) + \alpha_2 \Delta (T_2 \Delta \delta p) + \dots + \alpha_5 \Delta (T_H \Delta \delta p),$$

where the values of  $\alpha_1, \alpha_2, \dots, \alpha_5$  are generated by the Gaussian elimination process.

The expansion coefficients  $(C_{ij})$  are functions of the seven unknowns. The procedure of solution of  $\delta p$  is, therefore, as follows:

1. Calculate  $(C_{ij})$  using the latest iterate values  $x_1^l, x_2^l, \dots, T^l, p^l$ .
2. Perform Gaussian elimination on the system (Eq. 18) to obtain Eq. 21.
3. Solve Eq. 21 for  $\delta p$  using reduced band-width direct solution (Ref. 6).
4. Solve for  $\delta T, \delta S_w, \dots, \delta x_1$ , from the first

six equations of the system (Eq. 18). Calculate the latest iterates as

$$p^{\ell+1} = p_n + \delta p, T^{\ell+1} = T_n + \delta T, \text{ etc.}$$

This cycle is terminated when the maximums over all grid blocks of  $|\delta p^{\ell+1} - \delta p|$  and  $|\delta T^{\ell+1} - \delta T|$  are less than specified tolerances. Superscript  $\ell$  here is iteration number.

### SATURATION EQUATIONS

The use of explicit transmissibilities and explicit capillary pressure in Eqs. 1 through 7 leads to conditional stability of the solution. MacDonald and Coats<sup>7</sup> and later authors<sup>5,8</sup> proposed an implicit saturation calculation following the pressure-equation solution to eliminate this conditional stability. Ref. 5 describes an implicit calculation of water saturation with mention of a difficulty in calculating the gas saturation implicitly as well. We have resolved that difficulty to the extent that our current simultaneous, implicit solution for both saturations results in three to five times fewer time steps than the previous treatment.<sup>5</sup> Spillette *et al.*<sup>8</sup> recommended this simultaneous solution for two saturations in connection with black-oil modeling.

For clarity, we will describe this saturation calculation in the context of x-direction flow between three grid blocks denoted by  $i-1$ ,  $i$ , and  $i+1$ . Writing Darcy's law for each phase flow rate and eliminating the oil pressure gradient from the three equations gives the following fractional flow expressions:

$$q_w = \frac{T_w}{T} [q - (T_o + T_g) \Delta P_{cwo} - T_g \Delta P_{cgo} - (T_o \Delta \gamma_{wo} + T_g \Delta \gamma_{wg}) \Delta Z] \dots (22a)$$

$$q_o = \frac{T_o}{T} [q + T_w \Delta P_{cwo} - T_g \Delta P_{cgo} + (T_w \Delta \gamma_{wo} - T_g \Delta \gamma_{og}) \Delta Z] \dots (22b)$$

$$q_g = \frac{T_g}{T} [q + T_w \Delta P_{cwo} + (T_w + T_o) \Delta P_{cgo} + (T_w \Delta \gamma_{wg} + T_o \Delta \gamma_{og}) \Delta Z] \dots (22c)$$

Here,  $q_w$ ,  $q_o$ , and  $q_g$  denote the RB/D flow rates from Block  $i-1$  to Block  $i$ .  $\Delta P_c$  is  $P_{ci-i} - P_{ci}$ ,  $\Delta Z$  is  $Z_{i-1} - Z_i$ , and  $\Delta \gamma_{wg}$  is  $\bar{\gamma}_w - \bar{\gamma}_g$  (psi/ft), where  $\bar{\gamma}$  is interblock average fluid density.  $T$  is  $T_w + T_o + T_g$  and  $q$  is  $q_w + q_o + q_g$ . All transmissibilities here are  $(kA/\ell)(k_r/\mu)$ , where  $A$  is the area normal to flow and  $\ell$  is the distance between block centers.

With transmissibilities and capillary pressures evaluated at the old time level, Eqs. 22a through 22c yield the interblock flow rates corresponding to

the solution of Eqs. 1 through 7. We denote the saturation changes satisfying Eqs. 1 through 7 by  $\delta S_w^*$  and  $\delta S_g^*$ . The final saturation changes  $\delta S_w$  and  $\delta S_g$  satisfy the mass balance equations:

$$\delta q_{wi-1,i} - \delta q_{wi,i+1} = \frac{V}{\Delta t} \phi_{n+1} (\delta S_{wi} - \delta S_{wi}^*) \dots (23a)$$

$$\delta q_{oi-1,i} - \delta q_{oi,i+1} = \frac{V}{\Delta t} \phi_{n+1} (\delta S_{oi} - \delta S_{oi}^*) \dots (23b)$$

The  $\delta q$  terms are the perturbations in the interblock flows given by Eqs. 22a through 22c owing to changes in  $T_w$ ,  $T_o$ ,  $T_g$ ,  $P_{cwo}$ , and  $P_{cgo}$  over the time step. These perturbations can be expressed as

$$\delta q_{wi-1,i} = \frac{\delta q_w}{\delta S_{wi-1}} \delta S_{wi-1} + \frac{\delta q_w}{\delta S_{wi}} \delta S_{wi} + \frac{\delta q_w}{\delta S_{gi-1}} \delta S_{gi-1} + \frac{\delta q_w}{\delta S_{gi}} \delta S_{gi} \dots (24a)$$

$$\delta q_{oi-1,i} = \frac{\delta q_o}{\delta S_{wi-1}} \delta S_{wi-1} + \frac{\delta q_o}{\delta S_{wi}} \delta S_{wi} + \frac{\delta q_o}{\delta S_{gi-1}} \delta S_{gi-1} + \frac{\delta q_o}{\delta S_{gi}} \delta S_{gi} \dots (24b)$$

Substituting Eqs. 24a and 24b into Eqs. 23a and 23b and replacing  $\delta S_o$  by  $-\delta S_w - \delta S_g$ , we obtain two equations in the two unknowns  $\delta S_w$  and  $\delta S_g$ :

$$\Delta(T_{11} \Delta \delta S_w) + \Delta(T_{12} \Delta \delta S_g) = \frac{V}{\Delta t} \phi_{n+1} (\delta S_{wi} - \delta S_{wi}^*) \dots (25a)$$

$$\Delta(T_{21} \Delta \delta S_w) + \Delta(T_{22} \Delta \delta S_g) = \frac{V}{\Delta t} \phi_{n+1} (\delta S_{gi} - \delta S_{gi}^*) \dots (25b)$$

This Laplacian notation is only qualitative in that the actual form (in x-direction terms only) of, for example,  $\Delta(T_{11} \Delta \delta S_w)$  is  $a_{i+1} \delta S_{wi+1} + a_i \delta S_{wi} + a_{i-1} \delta S_{wi-1}$ , where the  $a$  values arise from Eqs. 24a and 24b and depend on the directions of phase flows. The transmissibilities in Eqs. 22a through

22c are based on upstream relative permeabilities. Thus, if all phases were flowing from Block  $i-1$  to Block  $i$  then, except for capillary pressure, the terms  $\delta q_w / \delta S_{wi}$ ,  $\delta q_w / \delta S_{gi}$ ,  $\delta q_o / \delta S_{wi}$ , and  $\delta q_o / \delta S_{gi}$  would be zero.

Eqs. 25a and 25b are solved simultaneously using the reduced band-width direct solution.<sup>6</sup> The coefficients  $\delta q_w / \delta S_{wi-1}$ , etc., are then re-evaluated as follows. Eqs. 22a through 22c can be expressed as

$$q_w = q_w(S_{wi-1}, S_{wi}, S_{gi-1}, S_{gi}) \quad (26a)$$

$$q_o = q_o(S_{wi-1}, S_{wi}, S_{gi-1}, S_{gi}) \quad (26b)$$

After solution of Eqs. 25a and 25b, we have the latest iterate values of the saturations,

$$S_{wi-1}^l, S_{wi}^l, S_{gi-1}^l, S_{gi}^l$$

The value of  $\partial q_w / \partial S_{wi-1}$  is calculated as

$$\frac{\partial q_w}{\partial S_{wi-1}} = \frac{q_w(S_{wi-1}^l, S_{wi,n}^l, S_{gi-1,n}^l, S_{gi,n}^l) - q_w(S_{wi-1,n}^l, S_{wi,n}^l, S_{gi-1,n}^l, S_{gi,n}^l)}{S_{wi-1}^l - S_{wi-1,n}^l} \quad (27)$$

Before the first solution of Eqs. 25a and 25b, the saturations are perturbed by a fixed amount. We have found two iterations to be sufficient. That is, Eqs. 25a and 25b are solved twice, with  $\Upsilon_{ij}$  values updated after the first iteration.

#### IMPLICIT PRODUCTION RATES

A conditional stability in the solution of Eqs. 1 through 7 arises owing to explicit treatment of the production rates  $q_w$ ,  $q_o$ , and  $q_g$ . In the pressure-equation solution,<sup>5</sup> these rates were represented implicitly in terms of  $\delta S_w$  and  $\delta S_g$  as well as  $\delta p$ . We have found the revised procedure described here to be simpler, more accurate, and equally conducive to stability.

For brevity, we will describe only the case of a well on deliverability producing from a single layer. As presented in Ref. 5, the production rate of phase  $m$  ( $m = w, o, g$ ) is

$$q_m = PI \cdot \frac{k_{rm}}{\mu_m} (p - p_{well}) \quad (28)$$

where  $p_{well}$  is the specified bottom-hole flowing well pressure and  $p$  is the reservoir grid-block

pressure calculated in the simulator equations. The rate is expressed implicitly in pressure as

$$q_m = q_{mn} + q_{m,p} \delta p \quad (29)$$

where

$$q_{mn} = PI \cdot \frac{k_{rnm}}{\mu_m} (p_n - p_{well}) \quad (30)$$

and

$$q_{m,p} = PI \cdot \frac{k_{rmp}}{\mu_m} \quad (31)$$

No implicit rate terms in saturation are used. The  $q_{mn}$  value is carried in the  $R_i$  term defined above and the  $q_{m,p}$  terms appear in the coefficients  $C_{i,7}$ .

After solution of the pressure and saturation equations, the total production rate,  $q$ , is  $q_w + q_o + q_g$  RB/D with the individual rates given by Eq. 29. These rates are adjusted to force the relative phase rates to obey the relative-permeability curves. The equations for this adjustment are

$$-qf_w + q_w = \frac{V}{\Delta t} \phi_{n+1} (\delta S_w - \delta S_w^*), \quad (32a)$$

and

$$-qf_g + q_g = \frac{V}{\Delta t} \phi_{n+1} (\delta S_g - \delta S_g^*), \quad (32b)$$

where  $\delta S_w^*$  and  $\delta S_g^*$  are the solutions to Eq. 18,  $\delta S_w$  and  $\delta S_g$  are the resulting adjusted saturation changes, and

$$f_w = \lambda_w / \lambda_T \quad f_g = \lambda_g / \lambda_T \quad (33)$$

The individual phase mobilities are expressed as

$$\begin{aligned} \lambda_w &= \lambda_{wn} + \lambda_w' \delta S_w \\ \lambda_g &= \lambda_{gn} + \lambda_g' \delta S_g \\ \lambda_o &= \lambda_{on} + \lambda_{ow}' \delta S_w + \lambda_{og}' \delta S_g \end{aligned} \quad (34)$$

where  $\lambda_w'$ ,  $\lambda_g'$ , etc., are chord slopes from the relative-permeability curves.

Substitution of Eqs. 33 and 34 into Eqs. 32a and 32b gives two nonlinear equations in the two unknowns  $\delta S_w$  and  $\delta S_g$ . These equations can be functionally represented as

$$F_1(x_1, x_2) = 0$$

$$F_2(x_1, x_2) = 0, \dots \dots \dots (35)$$

where  $x_1 \equiv \delta S_w$  and  $x_2 \equiv \delta S_g$ . Application of the Newton-Raphson procedure then gives the following equations for successive iterates.

$$F_{11}x_1^{\ell+1} + F_{12}x_2^{\ell+1} =$$

$$F_{11}x_1^\ell + F_{12}x_2^\ell - F_1(x_1^\ell, x_2^\ell), \dots \dots (36a)$$

$$F_{21}x_1^{\ell+1} + F_{22}x_2^{\ell+1} =$$

$$F_{21}x_1^\ell + F_{22}x_2^\ell - F_2(x_1^\ell, x_2^\ell), \dots \dots (36b)$$

where  $F_{ij} = \partial F_i / \partial x_j$  and  $\ell$  is the iteration number. The chord slopes  $\lambda_w, \lambda_g$ , etc., may or may not be re-evaluated between Newton-Raphson iterations. We have found little need for this re-evaluation.

After convergence of Eqs. 36a and 36b, the final production rates are calculated as

$$q_w = qf_w \quad q_o = qf_o \quad q_g = qf_g$$

where the fractional flows are calculated from Eqs. 33 and 34.

#### RELATIVE-PERMEABILITY TREATMENT

Two-phase water and oil relative-permeability curves at original reservoir temperature are read in tabular form vs water saturation. These water-oil relative-permeability curves are converted internally to normalized forms of  $\bar{k}_{rw}$  and  $\bar{k}_{row}$  vs  $\bar{S}_w$ , where

$$\bar{S}_w = \frac{S_w - S_{wir}(T_i)}{1 - S_{wir}(T_i) - S_{orw}(T_i)}$$

$$\bar{k}_{rw} = \frac{k_{rw}}{k_{rwro}(T_i)}$$

$$\bar{k}_{row} = \frac{k_{row}}{k_{rocw}(T_i)} \dots \dots \dots (38)$$

Values of  $S_{wir}, S_{orw}, k_{rwro}$ , and  $k_{rocw}$  are read in tabular form as functions of temperature. For a given temperature, interpolation is performed to obtain the current values of  $S_{wir}$ , etc. The current  $S_w$  value is then used to calculate  $\bar{S}_w$  followed by interpolation in the normalized relative-permeability table to obtain  $\bar{k}_{rw}$  and  $\bar{k}_{row}$ . Finally,  $k_{rw}$  and  $k_{row}$  are obtained by multiplication by  $k_{rwro}(T)$  and  $k_{rocw}(T)$ . Weinbrandt and Ramey<sup>9</sup> found from laboratory work that  $S_{wir}$  increased significantly

with temperature in water-oil systems.

Two-phase gas-oil relative-permeability curves at original reservoir temperature are read in tabular form as functions of total liquid saturation  $S_L = S_{wir} + S_o$ . The oil relative-permeability curve is then normalized as  $\bar{k}_{rog}$  vs  $\bar{S}_L$ , where

$$\bar{k}_{rog} = k_{rog} / k_{rocw}(T_i)$$

$$\bar{S}_L = \frac{S_o - S_{org}(T_i)}{1 - S_{wir}(T_i) - S_{org}(T_i)}$$

$k_{rog}$  is calculated for given values of  $T, S_w$ , and  $S_o$  as follows. Current values of  $S_{org}$  and  $S_{wir}$  are calculated at temperature  $T$ .  $\bar{S}_L$  is then calculated as  $[S_w + S_o - S_{wir}(T) - S_{org}(T)] / [1 - S_{wir}(T) - S_{org}(T)]$ .  $\bar{k}_{rog}$  is interpolated from the normalized  $\bar{k}_{rog}$  vs  $\bar{S}_L$  table and  $k_{rog}$  is then obtained by multiplication by  $k_{rocw}(T)$ .

Relative permeability to gas is obtained using both hysteresis and temperature-dependence considerations. Residual gas saturation, critical gas saturation, and relative permeability to gas at residual oil are all read in tabular form vs temperature. The originally read gas relative-permeability curve (at reservoir temperature) is normalized as  $\bar{k}_{rg}$  vs  $\bar{S}_g$ , where

$$\bar{k}_{rg} = k_{rg} / k_{rgro}(T_i)$$

$$\bar{S}_g = \frac{S_g - S_{gc}(T_i)}{1 - S_{org}(T_i) - S_{wir}(T_i) - S_{gc}(T_i)}$$

$$\bar{k}_{rg} = \frac{k_{rg}}{k_{rgro}(T_i)} \dots \dots \dots (39)$$

At a given temperature,  $T$ , and gas saturation,  $S_g$ ,  $k_{rg}$  is calculated as follows. Current residual gas saturation,  $S_{gr}(T)$ , is calculated. This is the residual gas saturation assuming a maximum gas-phase saturation of  $1 - S_{wir}(T_i) - S_{org}(T_i)$  has been reached at some previous time. The actual residual gas saturation used is

$$S_{gr}^* = \frac{S_{gmax}}{1 - S_{wir}(T_i) - S_{org}(T_i)}$$

$$\cdot S_{gr}(T), \dots \dots \dots (40)$$

where  $S_{gmax}$  is the maximum gas-phase saturation obtained in the grid block up to the current time. An effective residual gas saturation is next calculated as

$$S_{greff} = \omega S_{gr}^* + (1 - \omega) S_{gc}(T), \dots \dots \dots (41)$$

where weight factor,  $\omega$ , is

$$\omega = \frac{S_{gmax} - S_g}{S_{gmax} - S_{gr}^*} \dots \dots \dots (42)$$

Normalized gas saturation,  $\bar{S}_g$ , is calculated as  $(S_g - S_{gref})/[1 - S_{wir}(T) - S_{org}(T)]$ .  $\bar{k}_{rg}$  is obtained by interpolating in the table of  $\bar{k}_{rg}$  vs  $\bar{S}_g$  and  $k_{rg}$  is then obtained by multiplying by  $k_{rgro}$  (7).

This procedure achieves the following hysteretic character. As gas saturation rises with  $S_g = S_{gmax}$  each time step,  $k_{rg}$  will follow the originally read-in curve of  $k_{rg}$  vs  $S_g$  in spite of the fact that residual gas saturation,  $S_{gr}$ , is increasing. Then, if  $S_g$  decreases from  $S_{gmax}$ ,  $k_{rg}$  will follow smoothly a curve that exhibits a residual gas saturation decreasing continuously toward  $S_{gr}^*$  as  $S_g$  decreases toward  $S_{gr}^*$ . When  $S_g$  finally falls to  $S_{gr}^*$ ,  $\omega$  will be 1,  $S_{gref}$  will equal  $S_{gr}^*$ ,  $\bar{S}_g$  is 0, and  $\bar{k}_{rg} - k_{rg} = 0$ .

In all cases discussed above, geometric similarity of the relative-permeability curves is assumed regardless of temperature change. That is, only the end-point saturations and relative permeabilities are allowed to change with temperature; the normalized curves (for example,  $\bar{k}_{rw}$  vs  $\bar{S}_w$ ) are held invariant.

The relative permeability to oil,  $k_{ro}$ , is obtained from  $k_{rw}$ ,  $k_{row}$ ,  $k_{rog}$ , and  $k_{rg}$  using Stone's<sup>10</sup> method.

### MODEL RESULTS

Model results are compared below with the Willman *et al.*<sup>11</sup> laboratory steamflood of a partially distillable oil. Complete data and model results are given for a test problem that serves as a fairly

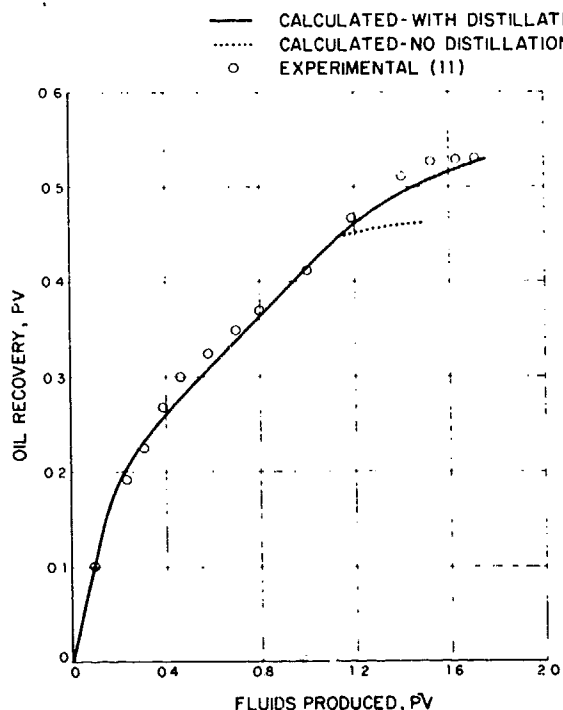


FIG. 1 -- COMPARISON OF CALCULATED WITH OBSERVED OIL-RECOVERY CURVES.

severe test of model stability. Results from 16 additional test-problem runs are listed and discussed to provide some insight into the effects of changes in and relative importance of various types of model input data. Finally, results and discussion are presented for a model application to a Cold Lake (Alta.) steam-injection test.

### WILLMAN EXPERIMENTAL DATA

Fig. 1 compares calculated oil recovery with the experimental recovery reported by Willman *et al.* for a laboratory steamflood. The oil used was 25-percent distillable Napoieum and 75-percent nondistillable Primol with a viscosity of 22.5 cp at the initial 80 °F temperature. The dotted line in Fig. 1 shows the model results reported previously<sup>5</sup> with no distillation calculations. Data used in the present calculation are identical with those reported previously.<sup>5</sup> Equilibrium  $K$  values used for Component 2 (Napoieum) were independent of pressure and varied with temperature as follows:

$T$ (°F)	$K_{Napoieum}$
80	0.00058
180	0.0028
280	0.008
380	0.024

Fig. 2 shows the specified variation of oil viscosity with composition.

Since both the Napoieum equilibrium  $K$  value and oil-viscosity composition dependence were not measured, we performed calculations for a range of these parameter values. The calculated oil recovery was insensitive to changes in specified variation of oil viscosity with composition. The dotted line in Fig. 2 shows a viscosity reduction twofold more than that of the solid line as  $x_3$  decreases from the original value of 0.531. The effect of this change on the calculated oil-recovery curve is indiscernible on the scale of Fig. 1.

The effect of  $K$  values on calculated recovery was significant. Calculated oil recovery at 1.6-PV produced fluids varied as follows with the value of  $K_{Napoieum}$  at 330 °F:

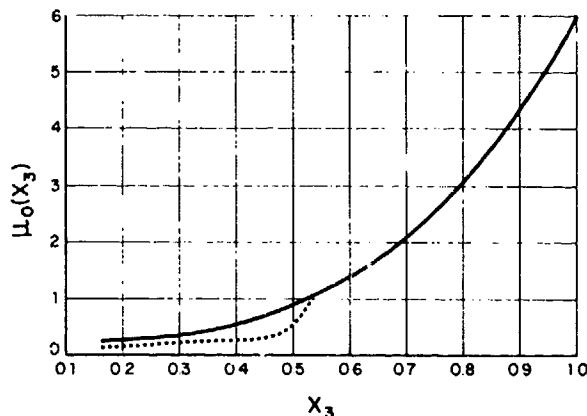


FIG. 2 -- OIL-VISCOSITY VARIATION WITH COMPOSITION.

$K_{\text{Napoleum}} (330^\circ\text{F})$	Pore Volume Oil Recovery at 1.6-PV Produced
0.012	0.498
0.016	0.515
0.02	0.53
0.18	0.595

These recoveries compare with an experimentally observed value of 0.526. Figs. 3 and 4 give some insight into the reason for this dependence on the  $K$  value. A higher  $K$  value results in more rapid and more complete vaporization of the distillable component behind the steam front. This, in turn, produces (1) a higher mol fraction of the distillable component in the condensing zone at the steam front, and (2) more shrinkage of the oil after residual oil saturation is reached by viscous displacement. It is this post-displacement shrinkage that yields

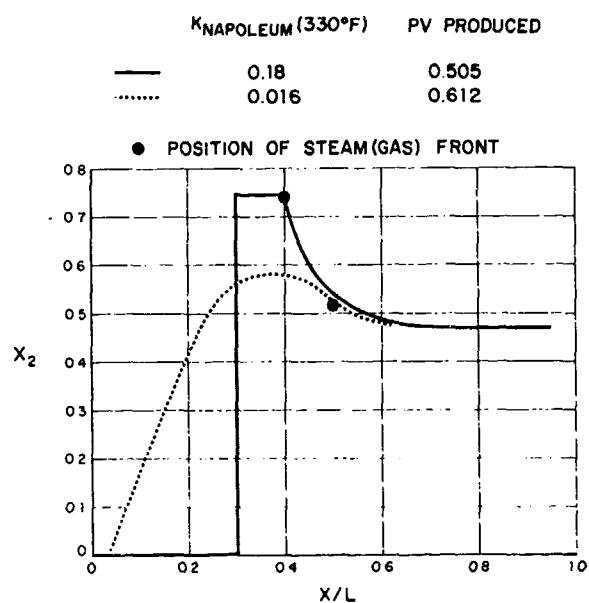


FIG. 3 — EFFECT OF DISTILLABLE COMPONENT  $K$  VALUE ON COMPOSITION PROFILE.

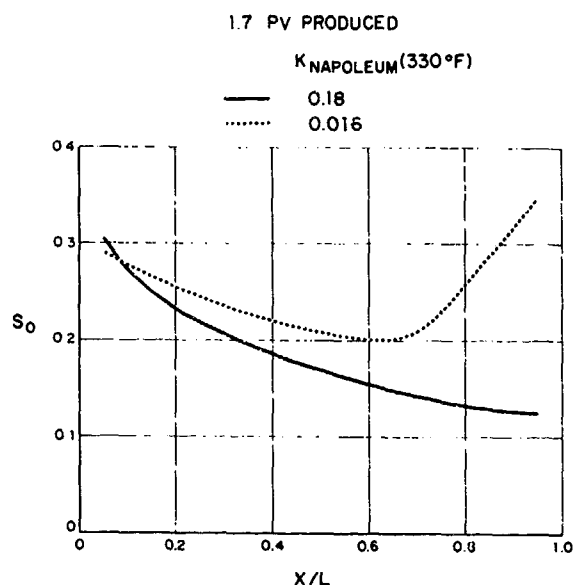


FIG. 4 — EFFECT OF DISTILLABLE COMPONENT  $K$  VALUE ON RESIDUAL OIL-SATURATION PROFILE.

the increased recovery. Fig. 4 shows the lower residual oil saturation corresponding to the greater recovery for the case of the higher  $K$  value. At 1.7-PV produced, the distillable component mol fraction ( $x_2$ ) is zero throughout the core for the  $K = 0.18$  case, while  $x_2$  varies from 0 at  $x/L = 0.7$  to 0.613 at  $x/L = 1$  for the  $K = 0.016$  case.

#### TEST PROBLEM

Table 1 gives model data for a two-dimensional cross-sectional test problem involving no distillation. We have used these data as a standard problem for evaluating different treatments of the implicit saturation equations described above. It is hoped that our inclusion of complete data and results will aid others in developing modeling approaches of greater stability and/or efficiency than reported here.

In brief, the problem is an  $x$ - $z$  slice 164 ft long, 115 ft wide, and 63 ft thick with an isotropic 4,000-md permeability. A  $4 \times 3$  ( $x$ - $z$ ) computational grid was used with a constant 37.5-B/D (cold water equivalent) injection rate of steam into the bottom layer. Calculations were carried to 1,800 days. Following an initial 1-day time step, automatic time-step selection was used with the new time step,  $\Delta t_{n+1}$ , selected as the lesser of  $(\Delta t_n \times 0.03/\text{DSMAX}, \Delta t_n \times 30/\text{DTEMPMAX})$ , where  $\Delta t_n$  is the previous time step and DSMAX and DTEMPMAX are the maximum saturation and temperature ( $^\circ\text{F}$ ) changes, respectively, over the grid in the last time step. Limitations of  $\Delta t_{n+1}/\Delta t_n \leq 1.5$ , and  $1 \leq \Delta t \leq 20$  days were imposed.

Fig. 5 shows computed oil recovery and instantaneous producing WOR (produced steam expressed as equivalent cold water) vs time. Ninety-three time steps were required to reach 1,000 days, 141 steps to 1,300 days, and 189 steps to 1,800 days. Computing time was 20.5 seconds CDC 6600 CPU time, or 0.009 seconds per grid block per time step. Table 2 gives pressure and fluid saturation arrays at 1,800 days.

#### SENSITIVITY RUNS

With the above test problem as a base case, a number of model runs were performed to study the sensitivity of results to changes in model data. While these sensitivity results are neither exhaus-

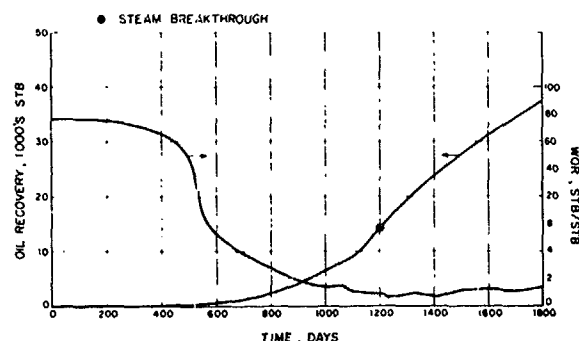


FIG. 5 — TEST-PROBLEM OIL-RECOVERY AND WOR VS TIME.

TABLE 1 — TEST-PROBLEM DATA

$NX = 4$     $NY = 1$     $NZ = 3$   
 $c_w = 3.1 \times 10^{-6}$   
 $c_o = 5 \times 10^{-6}$   
 $c_r = 8 \times 10^{-6}$   
 $C_{To} = 4.1 \times 10^{-4}$   
 $C_{p3} = 0.5$   
 $(\rho C_p)_R = 35$   
 Water density = 62.4 lb/cu ft at  $p_i, T_i$ .  
 Stock-tank oil density = 55 lb/cu ft.  
 $T_i = 90^\circ\text{F}$   
 $p_i = 75$  psia at 32.5 ft below top of formation.  
 Oil formation volume factor at  $p_i, T_i = 1.0$  RB/STB.

$T$ ( $^\circ\text{F}$ )	$\mu_o$	$\mu_w$	$\mu_s$
75	5,780	0.92	0.0095
100	1,380	0.681	0.0102
150	187	0.435	0.0115
200	47	0.305	0.0127
250	17.4	0.235	0.0138
300	8.5	0.187	0.0149
350	5.2	0.156	0.0158
500	2.5	0.118	0.0174

Reservoir thermal conductivity  $K_R = 38.4$ .  
 Overburden thermal conductivity  $K_{OB} = 38.4$ .  
 $(\rho C_p)_{OB} = 35$ .

Water-Oil Relative-Permeability Table

$S_w$	$k_{rwo}$	$k_{row}$
0.2	0	1
0.25	0.0102	0.7690
0.294	0.0168	0.7241
0.357	0.0275	0.6206
0.414	0.0424	0.5040
0.49	0.0665	0.3714
0.557	0.0970	0.3029
0.63	0.1148	0.1555
0.673	0.1259	0.0956
0.719	0.1381	0.0576
0.789	0.1636	0
1.0	1.0	0

Gas-Oil Relative-Permeability Table

$S_L = S_{wir} + S_o$	$k_{rog}$	$k_{rg}$
0.290	0.0000	0.1700
0.395	0.0294	0.1120
0.433	0.0461	0.1022
0.515	0.0883	0.0855
0.569	0.1172	0.0761
0.614	0.1433	0.0654
0.663	0.1764	0.0500
0.719	0.2170	0.0372
0.750	0.2255	0.0285
0.805	0.2919	0.0195
0.850	0.3373	0.0121
0.899	0.5169	0.0026
1.000	1.0000	0.0000

$P_{cwo} = 0$ .  
 $P_{cgo}$  = straight line from 3.0 at  $S_L = 0.29$  to -3.0 at  $S_L = 1.0$ .  
 Grid-block dimensions:  $\Delta x = 41$  ft,  $\Delta y = 115$  ft,  $\Delta z = 21$  ft.  
 $k_h = k_v = 4,000$  md.  
 $\phi_i = 0.38$ .  
 $S_{wi} = 0.30$ .  
 $S_{gi} = 0$ .  
 Well 1: Completed in grid block  $i = j = 1, k = 3$ .  
 Steam-injection rate = 37.5 B/D cold-water equivalent.  
 Steam quality = 0.7 at 200 psia.  
 Well 2: Completed in grid blocks  $i = 4, j = 1, k = 1, 2, 3$ .  
 PI = 900.  
 On deliverability against 60-psia bottom-hole pressure at center of top layer. Allocation of production among layers on basis of mobility and pressure.

tive nor necessarily applicable to other problems, they do provide some insight into the relative importance and effects of various types of required model data.

Table 3 lists oil recovery at 1,000 and 1,800 days, and steam breakthrough time for each of 17 model runs. We will discuss these results in the order they appear in the table.

A fivefold reduction in vertical permeability delayed steam breakthrough owing to a less pronounced steam override, but did not alter the oil-recovery curve. Oil recovery and breakthrough time were unaffected by reduction of the isotropic permeability from 4,000 to 2,000 md. Steam injection in the top 21 ft, as opposed to the bottom 21 ft, more than doubled oil production at 1,000 days but gave somewhat less oil recovery at 1,800 days. Breakthrough time decreased from 1,200 to 900 days.

The effect of a  $\pm 10$ -percent change in steam quality was significant with oil recovery increasing and breakthrough time decreasing with increasing quality. Reduction of initial water saturation from 0.30 to 0.25 (irreducible water saturation = 0.20) considerably increased oil recovery. The effect of a threefold increase in thickness, accompanied by a threefold injection-rate increase, was significantly increased oil recovery with faster steam breakthrough. The effect of injection interval was much greater with the 189-ft thickness than with the base-case 63-ft thickness. Injection in the top one-third as opposed to the bottom one-third of thickness only reduced recovery at 1,800 days from 66.4 percent oil originally in place to 65.1 percent for the 63-ft thickness. The reduction in recovery was from 78 percent to 65.7 percent for the 189-ft thickness at 1,800 days and from 50.7 to 30.5 percent at 1,000 days. A doubling of the injection rate significantly increased early recovery, compared with the base case at equal cumulative injection volumes, but only slightly increased the final recovery.

Reduction of the overburden thermal conductivity by a factor of 2 doubled recovery at 1,000 days and

TABLE 2 — TEST-PROBLEM PRESSURE AND SATURATION DISTRIBUTIONS AT 1,800 DAYS

		Oil Pressure at Grid-Block Center					
		$i$					
		1	2	3	4		
$k \downarrow$	Injection					Production	
	1	64.5	63.3	62.0	61.0		→
	2	64.9	63.6	62.3	61.2		
3	69.6	68.5	67.4	66.4			
Oil Saturation							
		0.0904	0.0905	0.0907	0.0911		
		0.1001	0.1091	0.1195	0.1196		
		0.3879	0.5530	0.6632	0.6770		
Water Saturation							
		0.2002	0.2002	0.2003	0.2004		
		0.2004	0.2005	0.2008	0.2012		
		0.2377	0.2387	0.2609	0.2660		
Steam Saturation							
		0.7094	0.7093	0.7090	0.7085		
		0.6995	0.6904	0.6797	0.6792		
		0.3745	0.2083	0.0759	0.0570		

significantly increased recovery at 1,800 days. The same significant effect on recovery followed from use of temperature-dependent relative permeability. The latter data change consisted of specifying a linear increase in  $S_{wir}$  from 0.20 at 90 °F to 0.50 at 350 °F. Increasing stock-tank oil density from 55 to 61 lb/cu ft resulted in a small decrease from 66.4- to 64.5-percent recovery at 1,800 days. Reducing the oil thermal expansion coefficient by a factor of 2 slightly reduced oil recovery.

#### STEAM-INJECTION TEST

Samoil<sup>12</sup> reported results of a 1965 steam-injection test in a Cold Lake (Alta.) formation. The 10 °API oil has a viscosity of about 100,000 cp at the 55 °F reservoir temperature. The unconsolidated, 4- to 14-darcy Cummings sand is 1,350 ft deep and consists of about 100 ft of oil sand and a 15-ft transition zone underlain by 25 ft of water. Measurements of sample porosities at 200- and 1,300-psi overburden pressures yield an effective calculated pore-volume compressibility ( $c_r$ ) ranging from 0.0001 to 0.000125 vol/vol/psi. This is roughly 30 times higher than formation compressibilities commonly used for consolidated sandstones or limestones.<sup>13</sup>

Steam was injected for 6 days at a wellhead injection pressure increasing from 800 to 970 psig. Cumulative injection was 8,400 bbl cold water equivalent. The well was perforated in the 30- to 100-ft interval below top of porosity. Table 4 gives model data used in simulating this steam injection test. The model was run in  $r$ - $z$ , single-well mode using small radial increments near the well as is common in coning calculations.

Following is a summary of calculated steam-injection volumes showing the effects of various parameters.

Run	Description	Cumulative Injection (bbl Cold Water Equivalent)
1	Base case - Table 4	840
2	$c_r = 0.000135$	4,064
3	$k = 7,000$ md	3,836
4	$k = 9,000$ md	6,458
5	Quality = 0.15	10,004
6	Quality = 0.45	4,422
7	$k_r$ temperature dependence	1,381
8	$S_{wi} = 0.36$	10,394
9	$S_{wi} = 0.36, c_r = 4 \times 10^{-6}$	2,691

The base case used a horizontal permeability of 8,000 md, a  $k_v/k_h$  ratio of 0.1, assumed bottom-hole quality and injection pressure of 0.3 and 900 psia, respectively, and a rock compressibility of 0.000004 vol/vol/psi. The resulting injection of 840 bbl is 10 times less than observed. Changing only rock compressibility, to 0.000135, increased the calculated injection to 4,064 bbl, which compares far better with the observed 8,400 bbl. The remaining runs listed used  $c_r = 0.000135$ .

Variation of horizontal permeability, retaining the  $k_v/k_h$  ratio of 0.1, showed a highly nonlinear increase of calculated injection volume with increasing permeability. Sensitivity to injected steam quality was also significant, with calculated injection volume increasing greatly with reduced quality and increasing slightly with increased quality. The temperature dependence specified was a rise of  $S_{wir}$  from 0.35 at 55 °F to 0.50 at 545 °F. The drastically reduced calculated injection volume resulted from the loss in water mobility in the injection grid blocks as temperature increased.

An increase of initial water saturation in the oil zone from the irreducible 0.35 to 0.36 increased the calculated injection from 4,064 (Run 2) to 10,394

TABLE 3 — SUMMARY OF SENSITIVITY RESULTS

Run	Description	Oil Recovery, Percent Oil Originally in Place		Steam Breakthrough Time (days)
		1,000 Days	1,800 Days	
1	Base-case test problem	11.6	66.4	1,210
2	$k_v = 800$ md	11.7	66.9	1,400
3	Injection in top 21 ft	25.9	65.1	900
4	Steam quality = 0.6	7.5	56.2	1,410
5	Steam quality = 0.8	17.2	71.3	1,080
6	$S_{wi} = 0.25$	18.7	73.8	1,210
7	Thickness - 189 ft, <sup>†</sup> injection in bottom 63 ft	50.7	78.0	850
8	Thickness - 189 ft, <sup>†</sup> injection in top 63 ft	30.5	65.7	350
9	Injection rate - 75 B/D	15.5 <sup>**</sup>	67.9 <sup>†</sup>	540
10	$K_{OB} = 19.2$	23.3	73.1	1,010
11	$k_r$ temperature dependence	24.3	72.3	1,250
12	Stock-tank oil density - 61 lb/cu ft	11.5	64.5	1,180
13	$C_{T_o} = 0.0002$	9.4	64.6	1,200
14	Distillation	12.1	67.9	1,200
15	$K$ values doubled	13.1	71.6	1,200
16	$\mu_o(x_3)$ halved for $x_3 < x_3$ initial	12.2	68.2	1,200
17	$[\mu_o(x_3) - 1]$ halved for $x_3 > x_3$ initial	12.0	68.3	1,200

\* Injection rate = 112.5 B/D cold-water equivalent, five layers of 21, 42, 63, 31.5, 31.5 ft used.

\*\* Time = 500 days.

† Time = 900 days.

bbl. This pronounced effect of only a 1-percent change in initial water saturation reflects the fact that water mobility at 0.36 saturation is about 250 times higher than initial, cold oil mobility. The final run shows that even with initially mobile water present, the effect of formation compressibility is still pronounced.

## CONCLUSIONS

A previously described three-dimensional steam-flood model<sup>5</sup> has been extended to account for steam distillation, solution gas, and temperature-dependent relative permeability. The more implicit calculation

of fluid saturations described above has increased model stability significantly relative to the earlier model.

The model gives a oil-recovery curve in moderately good agreement with experimental data obtained from a steamflood of a distillable oil. However, the model results are sensitive to the values of distillable-component equilibrium  $K$  values, and these were not measured.

Model input data and computed results given for a test problem should aid evaluation of other model formulations or solution techniques.

Sensitivity of calculated oil recovery to reservoir-fluid parameters was investigated using the test problem as a base case. Of the parameters studied, steam quality, initial water saturation, and temperature dependence of relative permeability had the greatest effect on oil recovery. The calculated recovery increased with increasing quality and decreasing initial water saturation. Inclusion of distillation effects for this problem resulted in only moderately increased oil recovery. The magnitude of this increase significantly depends on the values of the distillable-component equilibrium  $K$  values. For the base-case, 63-ft-thick formation, oil recovery was insensitive to the vertical location of the steam-injection interval. For a 189-ft-thick formation, recovery was considerably accelerated and higher with injection in the bottom as opposed to the top 63 ft.

In a 1965 steam-injection test in the Cold Lake area, 8,400 bbl of steam were injected in 6 days. Crude viscosity at original reservoir temperature was 100,000 cp. Injection volumes calculated using the model ranged from 840 to 10,394 bbl. Changing only formation compressibility, from  $4 \times 10^{-6}$  to  $1.35 \times 10^{-4}$ , increased calculated injection from 840 to 4,064 bbl. Independent measurement of this compressibility yielded values from  $1 \times 10^{-4}$  to  $1.25 \times 10^{-4}$ . Calculated injection volume increased greatly with increased permeability, decreased quality, and increased initial (mobile) water saturation. The increased formation compressibility had a strong effect on injection volume regardless of whether initial water saturation was irreducible or mobile.

TABLE 4 — STEAM-INJECTION TEST DATA

$c_w = 3.3 \times 10^{-6}$   
 $c_o = 10^{-5}$   
 $c_r = 4 \times 10^{-6}$   
 $C_{T_o} = 5 \times 10^{-4}$   
 $C_{p3} = 0.5$   
 $(\rho C_p)_R = 35$   
 Water density = 65 lb/cu ft at  $p_i, T_i$ .  
 $T_i = 55^\circ \text{F}$ .  
 $p_i = 410$  psia 115 ft below top of formation.  
 Stock-tank oil density = 62.14 lb/cu ft.  
 Oil FVF at  $p_i, T_i = 1.0$  RB/STB.

$T$ (°F)	Oil Viscosity (cp)	Water Viscosity (cp)	Steam Viscosity (cp)
55.0	100,000.0000	1.0000	0.0090
100.0	9,700.0000	0.6810	0.0102
210.0	135.0000	0.2910	0.0129
250.0	46.0000	0.2350	0.0138
300.0	19.8000	0.1870	0.0149
400.0	5.7000	0.1460	0.0152
500.0	2.2000	0.1260	0.0197
600.0	1.0000	0.1100	0.0250

$K_R = K_{OB} = 38.4$ .  
 $(\rho C_p)_{OB} = 35$ .

### Water-Oil

$S_w$	$k_{rw}$	$k_{roil}$	$P_{cwo}$
0.35000	0.00000	0.80000	0.3000
0.40000	0.01000	0.52000	0.2769
0.50000	0.04000	0.24000	0.2308
0.60000	0.07200	0.11000	0.1846
0.70000	0.12500	0.03200	0.1385
0.80000	0.20000	0.00000	0.0923
0.90000	0.35000	0.00000	0.0462
1.00000	1.00000	0.00000	0.0000

### Gas-Oil

$S_L$	$S_{wir} + S_o$	$k_{rR}$	$k_{rOG}$
0.45000		0.20000	0.00000
0.50000		0.14000	0.01700
0.60000		0.07200	0.06800
0.70000		0.04000	0.15800
0.80000		0.02000	0.30000
0.90000		0.00500	0.50000
1.00000		0.00000	0.80000

Wellbore radius  $r_w = 0.583$  ft.

Exterior radius  $r_e = 800$  ft.

$k_h = 8,000$  md.

$k_v = 800$  md.

$\phi_i = 0.36$ .

Grid:  $NX = 6, NZ = 8$ .

Layer thicknesses = 15, 15, 15, 15, 20, 20, 15, 25 ft.

Water-oil contact with  $P_{cwo} = 0$  at 115 ft from top of formation.

Bottom-hole injection pressure = 900 psia.

Steam quality = 0.3 at 900 psia.

## NOMENCLATURE

- $c$  = compressibility, vol/vol-psi  
 $C_p$  = specific heat, Btu/lb-°F  
 $c_r$  = rock formation compressibility  
 $(\rho C_p)_R$  = reservoir formation specific heat, Btu/cu ft rock-°F  
 $C_T$  = thermal expansion coefficient, vol/vol-°F  
 $f$  = fractional flow  
 $H$  = enthalpy, Btu/mol  
 $k, k_h$  = horizontal permeability, md  
 $k_r$  = relative permeability  
 $k_{rG}$  = relative permeability to gas

$k_{ro}$  = relative permeability to oil in three-phase system  
 $k_{rgrO}$  = relative permeability to gas at residual oil  $S_{org}$   
 $k_{rocw}$  = relative permeability to oil at irreducible water saturation  $S_{wir}$   
 $k_{rog}$  = relative permeability to oil in gas-oil two-phase system with irreducible water present  
 $k_{row}$  = relative permeability to oil in water-oil two-phase system  
 $k_{rw}$  = relative permeability to water  
 $k_{rwro}$  = relative permeability to water at residual oil  $S_{orw}$   
 $k_v$  = vertical permeability, md  
 $K_{OB}$  = thermal conductivity of overburden  
 $K_R$  = thermal conductivity of reservoir formation, Btu/°F-ft-D  
 $K_1, K_2$  = equilibrium  $K$  values for hydrocarbon components 1, 2  
 $L$  = core length, ft  
 $NX, NY, NZ$  = numbers of grid blocks in  $x$ ,  $y$ , and  $z$  directions  
 $p$  = oil pressure, psia  
 $p_{cgo}$  = gas-oil capillary pressure,  $p_g - p$   
 $p_{cwo}$  = water-oil capillary pressure,  $p - p_w$   
 $p_i$  = initial reservoir pressure  
 $p_{sat}$  = steam saturation pressure  
 $p_w, p_g$  = water- and gas-phase pressures  
 $PI$  = productivity index — see Ref. 5  
 $q_H$  = enthalpy production rate,  $q_w \rho_w H_w + q_o \rho_o H_o + q_g \rho_g H_g$ , Btu/D  
 $q_L$  = heat loss rate, Btu/D  
 $q_w, q_o, q_g$  = phase production rates, RB/D  
 $R$  = gas-law constant, 10.73 psia-cu ft/mol-°R  
 $S$  = fluid saturation, fraction  
 $S_{gc}$  = critical gas saturation  
 $S_{gi}$  = initial gas saturation  
 $S_{gr}$  = residual gas saturation  
 $S_{org}$  = residual oil saturation to gas in gas-oil irreducible water system  
 $S_{orw}$  = residual oil saturation to water in water-oil system  
 $S_{wi}$  = initial water saturation  
 $S_{wir}$  = irreducible water saturation  
 $t$  = time, days  
 $\Delta t$  or  $\Delta t_n$  = time step,  $t_n - t_{n-1}$ , days  
 $T$  = temperature, °F  
 $T_i$  = initial reservoir temperature  
 $U$  = internal energy, Btu/mol  
 $V$  = grid-block volume,  $\Delta x \cdot \Delta y \cdot \Delta z / 5.6146$ , res bbl  
 $x, y, z$  = Cartesian coordinates, ft

$x_i$  = mol fraction of hydrocarbon component  $i$  in the oil phase  
 $y_i$  = mol fraction of hydrocarbon component  $i$  in the gas phase  
 $y_s$  = mol fraction of steam in the gas phase  
 $z$  = gas phase compressibility factor  
 $Z$  = depth, measured vertically downward, ft  
 $\gamma$  = specific weight, psi/ft  
 $\delta$  = time difference operator; for example,  $\delta T = T_{n+1} - T_n$   
 $\rho$  = molar density, mol/RB  
 $\mu$  = viscosity, cp  
 $\phi_i$  = porosity, fraction  
 $\phi_i$  = porosity, at  $p_i$   
 $\lambda$  = mobility,  $k_r/\mu$   
 $\lambda_T$  = total mobility,  $\lambda_w = \lambda_o + \lambda_g$   
 $\Upsilon$  = transmissibility  
 $\Upsilon_c$  = heat-conduction transmissibility  
 $\Upsilon_H = \Upsilon_w H_w + \Upsilon_o H_o + \Upsilon_g H_g$   
 $\Upsilon_{H_2O} = \Upsilon_w + \Upsilon_g y_s$   
 $\Upsilon_i = \Upsilon_o x_i + \Upsilon_g y_i$ ,  $i = 1, 2, 3$  hydrocarbon components

#### SUBSCRIPTS

$g$  = gas  
 $i$  = hydrocarbon component number ( $x_i, y_i$ ) or initial ( $p_i, T_i$ )  
 $n$  = time level  
 $o$  = oil  
 $OB$  = overburden  
 $s$  = steam  
 $w$  = water

#### DIFFERENCE OPERATORS

$$\Delta(T_w \Delta p_w) = \Delta_x(T_w \Delta_x p_w) + \Delta_y(T_w \Delta_y p_w) + \Delta_z(T_w \Delta_z p_w)$$

$$\Delta_x(T_w \Delta_x p_w) = T_{wi+1/2, j, k} (p_{wi+1, j, k} - p_{wi, j, k}) - T_{wi-1/2, j, k} (p_{wi, j, k} - p_{wi-1, j, k})$$

Here,  $i, j$ , and  $k$  are grid-block indices;  $x = i\Delta x$ ,  $y = j\Delta y$ , and  $z = k\Delta z$ .

#### REFERENCES

1. Shutler, N. D.: "Numerical Three-Phase Simulation of the Linear Steamflood Process," *Soc. Pet. Eng. J.* (June 1969) 232-246; *Trans.*, AIME, Vol. 246.
2. Shutler, N. D.: "Numerical Three-Phase Model of the Two-Dimensional Steamflood Process," *Soc. Pet. Eng. J.* (Dec. 1970) 405-417; *Trans.*, AIME, Vol. 249.
3. Abdalla, A. and Coats, K. H.: "A Three-Phase, Experimental and Numerical Simulation Study of the Steamflood Process," paper SPE 3600 presented at the SPE-AIME 46th Annual Fall Meeting, New Orleans, La., Oct. 3-6, 1971.
4. Weinstein, H. G., Wheeler, J. A., and Woods, E. G.: "Numerical Model for Steam Stimulation," paper SPE 4759 presented at the SPE-AIME Third Improved Oil Recovery Symposium, Tulsa, April 22-24, 1974.

5. Coats, K. H., George, W. D., Chu, Chieh, and Marcum, B. E.: "Three-Dimensional Simulation of Steam-flooding," *Soc. Pet. Eng. J.* (Dec. 1974) 573-592; *Trans., AIME*, Vol. 257.
6. Price, H. S. and Coats, K. H.: "Direct Methods in Reservoir Stimulation," *Soc. Pet. Eng. J.* (June 1974) 295-308; *Trans., AIME*, Vol. 257.
7. MacDonald, R. C. and Coats, K. H.: "Methods for Numerical Simulation of Water and Gas Coning," *Soc. Pet. Eng. J.* (Dec. 1970) 425-436; *Trans., AIME*, Vol. 249.
8. Spillette, A. G., Hillestad, J. G., and Stone, H. L.: "A High-Stability Sequential Solution Approach to Reservoir Simulation," paper SPE 4542 presented at the SPE-AIME 48th Annual Fall Meeting, Las Vegas, Nev., Sept. 30-Oct. 3, 1973.
9. Weinbraudt, R. M. and Ramey, H. J., Jr.: "The Effect of Temperature on Relative Permeability of Consolidated Rocks," paper SPE 4142 presented at the SPE-AIME 47th Annual Fall Meeting, San Antonio, Tex., Oct. 8-11, 1972.
10. Stone, H. L.: "Estimation of Three-Phase Relative Permeability and Residual Oil Data," paper presented at the 24th Annual Technical Meeting of CIM, Edmonton, Alta., Canada, May 8-12, 1973.
11. Willman, B. T., Valleroy, V. V., Runberg, G. W., Cornelius, A. J., and Powers, L. W.: "Laboratory Studies of Oil Recovery by Steam Injection," *J. Pet. Tech.* (July 1961) 681-690; *Trans., AIME*, Vol. 222.
12. Samoil, L. L.: "A Field Experiment in Recovery of Heavy Oil Cold Lake, Alberta," paper presented at 17th Annual Meeting of CIM, 1966.
13. Hall, H. N.: "Compressibility of Reservoir Rocks," *Trans., AIME* (1953) Vol. 198, 309-314.

\*\*\*